Coolability of a corium pool in a debris bed – Critical heat flux (CHF) dependency with tilting angle, debris size and steam flowrate

C. Sartoris, Thierry Garcin, Florian Fichot

COOLABILITY OF A CORIUM POOL IN A DEBRIS BED – CRITICAL HEAT FLUX (CHF) DEPENDENCY WITH TILTING ANGLE, DEBRIS SIZE AND STEAM FLOWRATE

Sartoris C., Garcin T., and Fichot F.
Institut de Radioprotection et de Sureté Nucléaire
Cadarache, 13115, BP3, Saint Paul lez Durance
christine.sartoris@irsn.fr; thierry.garcin@irsn.fr; florian.fichot@irsn.fr

ABSTRACT

In case of severe accident in a light water reactor, large debris beds may form inside the core. If, in some part of the debris bed, the temperature increases up to the fuel melting point, it will lead to the formation and expansion of a molten pool which becomes more and more difficult to cool down as it grows. Therefore, it is of primary interest to determine the maximum size of a molten pool surrounded by debris which may be stabilized under water either after reflooding the vessel (as in TMI-2) or in case of a debris bed formed in a flooded reactor pit. One of the key parameters for that issue is the maximum heat flux (CHF) that may be extracted from the pool by water flowing within the debris bed. To determine that CHF, a series of tests have been conducted at IRSN. A heated copper cylinder generates a heat flux at one of its ends which simulates the boundary of the pool and is placed in contact with a debris bed made of monodisperse steel balls. Temperature measurements along the cylinder allow to calculate the heat flux transmitted to the debris bed through the cylinder tip.
Several experimental parameters have been investigated:

- The tilting angle of the heated surface, to take into account the shape of the molten pool.
- The diameter of the balls.
- The upwards steam flowrate simulating the steam coming from the part of the core located below the molten pool.
- The upwards liquid flowrate simulating the natural circulation of water along the debris bed.

As it is usual for CHF experiments, a significant dispersion of the measurements was observed, due to unavoidable evolutions of the contact zone between the copper surface and the balls. However, the impact of that random dispersion could be reduced by performing a large number of tests. This allows to identify clear tendencies on the CHF for the 3 studied parameters, with a rather good degree of confidence.
From those tendencies, it was possible to derive a general CHF correlation with the tilting angle and the steam flowrate. When the liquid velocity increases, the CHF increases in most cases, except for some cases with low velocity. However it is more difficult to find a clear correlation with the liquid velocity or flow rate.

KEYWORDS
Severe accidents, Corium coolability, Critical Heat Flux, Tilting angle, Steam Flowrate

1. INTRODUCTION

In case of a severe accident in a nuclear reactor, a large debris bed may be created in the core. If, in some part of this debris bed, the temperature keeps on rising up to the melting point, it may form a molten pool

of corium, as it happened in TMI-2 (Broughton et al., 1989). The molten pool is expected to become less and less coolable as it grows larger because the heat flux at the periphery of the pool increases linearly with the pool diameter. Therefore, it is of primary interest to determine the maximum size of a molten pool surrounded by debris which may be stabilized under water after reflooding the vessel (as in TMI-2) or in case of a debris bed formed in a flooded reactor pit (as in Nordic BWR for examples). The maximum heat flux that may be extracted, or Critical Heat Flux (CHF), is a key parameter to that issue. The open literature related to CHF along a heated plate immersed in a debris bed is much more limited than the one concerning CHF along a heated plate in a water pool.

(Fukusako et al., 1986) studied the transition and film boiling regimes for a cylindrical copper mass abutting a tank filled with a fluid and spherical balls. Several fluids, ball materials and ball diameters were considered. The heating surface is horizontal and about 50 mm in diameter. It is shown that the CHF increases with the ball diameter. For the smallest ball diameters, the heat flux monotonously rises with surface temperature, going from nucleate boiling to film boiling without any peak value. Correlations are given for transition and film boiling heat transfer coefficients (HTC) and for the minimum heat flux for larger balls. It is interesting to notice that correlations for film boiling and minimum heat transfer are directly derived from correlations established earlier for pool boiling, with a substitution of the hydraulic diameter by the ball diameter.

(Spencer, 2016) studied the heat transfer between a vertical steel wall and a volume filled with water and steel balls. Such situation might occur when a corium pool resulting from a severe accident in a CANDU reactor is in direct contact with the steel wall separating the calandria vessel from the shielding compartment. The author measured the heat transfer up to the point where CHF is achieved and is followed by a dramatic decrease. The experimental apparatus consists in a thick vertical copper heating plate in contact with a tank filled with saturated water and 11.1 mm steel balls. A wavy interface between the vapor rising along the surface and the liquid water is evidenced in the ball bed and surface aging phenomenon is observed. The author investigates in particular the dependence of CHF on the elevation along the heated plate: a best fit CHF correlation is proposed, with a decrease of CHF when elevation increases. More recently, the same author investigated the effect of the ball diameter in the same facility (Spencer, 2022). He could identify an increasing CHF with the ball diameter, with a rather clear correlation.

(Tung & Dhir, 1990) designed an experiment with a heated 19 mm stainless steel sphere embedded in a porous medium composed of spherical glass particles, with Freon-113 as a coolant fluid. The particles size varies from 2.9 mm to 19 mm. Asin (Fukusako et al., 1986), the authors observe that the CHF value decreases with decreasing particle size.

(Wang & Beckermann, 1993a, 1993b) derived a model for the dry-out heat flux along a plate in contact with a capillary porous medium. Their result shows that the non-dimensional CHF varies as the square root of the Peclet number.

In none of these works are the effect of surface orientation or the effect of steam flowrate. The effect of the liquid flowrate was not investigated experimentally either (although it is investigated numerically by (Wang & Beckermann, 1993a, 1993b), in the case of a vertical wall). But the effect of flow rate was widely studied for situations where there are no particles covering the heated plate. In particular, it was studied as a function of the tilting angle by (Park et al., 2018; Rougé, 1997; Sulatskii et al., 1997; Yoon et al., 2019). From those studies, it appears that the steam flow at the surface occurs only in a thin layer, comparable to a slug flow. The thickness of that layer depends on the tilting angle and on the liquid velocity. In all those studies where particles are absent, the CHF increase with the inlet liquid flow rate. However, the dependence is not straightforward, as it is modified by the other parameters also (in particular the tilting angle).

In the present work, the corium pool (a section of the pool actually) is simulated by a copper plate which can be tilted in order to describe different sections of the corium pool (see Fig. 1). A de-ionized water tank filled with steel balls stands for the debris bed. The CHF values are measured for 2 mm and 4 mm ball diameters. The choice of debris size was made according to observations made in the core debris

formed during TMI-2 accident (Broughton et al., 1989), and according to more fundamental considerations about fragmentation of fuel pellets (Coindreau et al., 2013). For each ball diameter, the effects of surface tilting, upcoming steam flow and upwards liquid flow are studied. CHF correlations depending on tilting angle and gas flow rate are derived from the experimental results. The comparison with pure water conditions will be led in a future work.

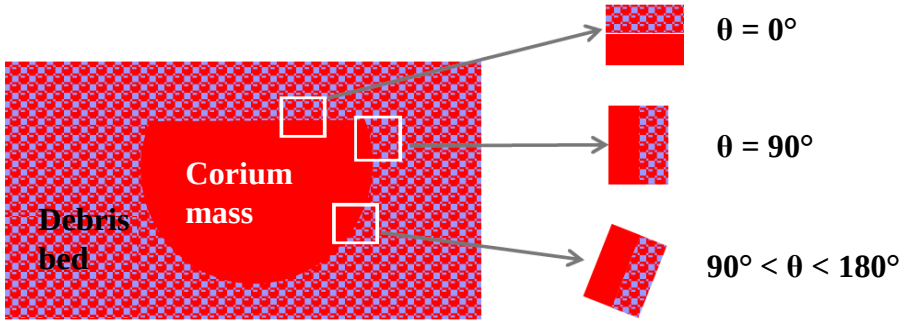

Figure 1. Description of the Contact Surface between Corium Mass and Debris Bed.

2. EXPERIMENTAL APPARATUS

The objective of the experiments is to measure the CHF on a flat surface in contact with a monodisperse steel ball bed at atmospheric pressure.
The heated surface is the end of a heated 50 mm diameter copper cylinder. This cylinder is heated by electrical cartridges at the other end. It comes in contact with a bed filled with steel balls and deionized water. The steel balls diameter may be either 2 mm or 4 mm. The bed is surrounded by a volume containing deionized saturated water acting as a temperature regulation for the balls bed and a water level regulator as it communicates with the ball bed (Fig. 2).

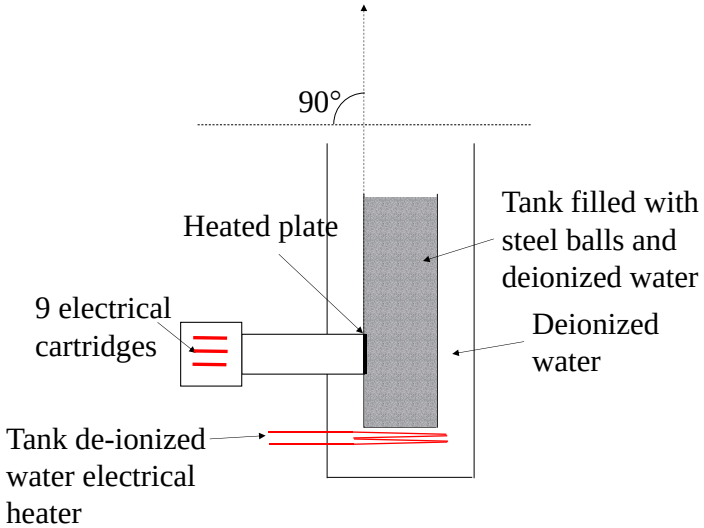

Figure 2. Schematic of the "VP" Test Section.

The influence of the heated surface tilting angle is studied. To that purpose, the whole Vertical Plate ("VP") test section may be tilted so that the initial angle of 90° corresponding to a vertical surface is successively brought to 120°, sometimes 135°, and 150°.

For the tests involving a steam or liquid flowrate, the "SG" test section is used (Fig. 3). This section is the same as the previous one but for a steam generator (SG) situated under the heated surface and composed of a copper parallelepiped heated with electrical cartridges, according to the same principle as the "heated plate" device. The flowrate produced by the SG is calculated as:

$$\text{Qsteam} = \frac{P}{Hls} \tag{1}$$

with P being the electrical power injected in the SG minus the thermal loss recorded, and H_{ls} the vaporization enthalpy. This calculated flowrate was comforted by measurement of the level decrease during vaporization in the "VP" test section.

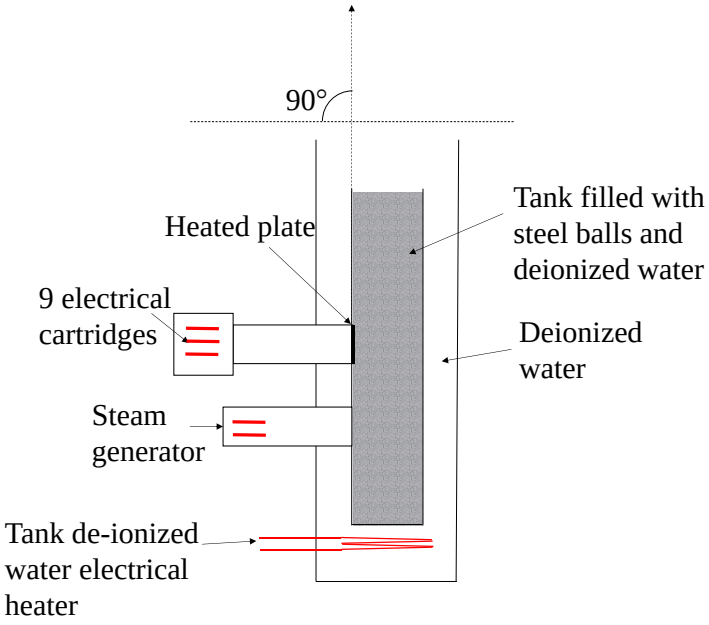

Figure 3. Schematic of the "SG" Test Section.

As this type of steam generator may also experience its own boiling crisis, unwelcomed boiling crisis may occur and prevent from achieving targeted steam flowrates. To avoid this unwanted phenomenon, larger balls are located in front of the steam generator surface to allow higher steam flowrates (Fig. 4). For a ball bed filled with 4 mm balls (resp. 2 mm), 8 mm balls (resp. 4 mm) are positioned in front of the SG. This is not the case for the additional series of tests with liquid flowrate ; for these tests, the bed is filled with mono-dimensional balls, either 2 mm balls or 4 mm balls. When steam is also injected in addition to the liquid, the steam flowrate is therefore limited by the steam generator CHF which depends on tilting angle and ball diameter.

Figure 4. Inside View of the Ball Bed Progressive Filling – Empty (Left), Large 8 mm Balls in front of SG (Center) and 4 mm Balls in the Rest of the Bed (right: picture is taken before the complete filling up to the heated plate).

It is also possible to inject thermalized deionized water at the bottom of the SG test section so that an upward liquid flowrate can be imposed in the ball bed.

The heated plate, steam generator and the surrounding volume are thermally insulated.

3. INTRUMENTATION, MEASURES AND HEAT FLUX CALCULATION

The heated cylinder is equipped with at least twelve 1 mm-diameter type K thermocouples, positioned along the four azimuths. They are used to estimate the heat flux transferred to the debris bed (see Fig. 5).

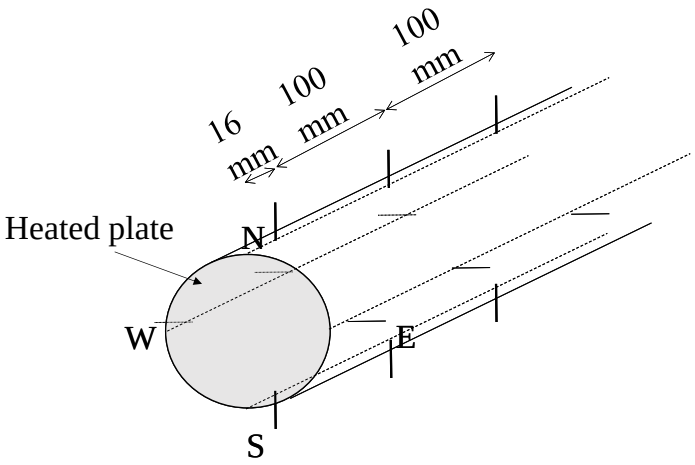

Figure 5. Implantation of the Twelve Thermocouples inside the heated cylinder.

Other type K thermocouples and PT100 sensors are positioned in the balls bed at about a few centimeters in front of the heated plate and in the channel to check the water saturation. The electrical power is supplied to the heating cartridges by a power regulator and an acquisition system collects the measured temperatures.
For each azimuth, the heat flux is derived from the temperature measurement of the two extreme thermocouples by Fourier's law:

$$\Phi = \frac{\lambda}{e}.(T_1 - T_2) \quad (2)$$

with λ being the copper thermal conductivity ($W.m^{-1}.K^{-1}$), e the distance (200 mm) between the thermocouples giving the temperatures T_1 and T_2 (K).
The value of the heat flux varies with the azimuth. In the following, the heat flux values correspond to the east-west averaged value.

4. SURFACE PREPARATION AND HEATING PROCEDURE

The surface is initially polished until a roughness of about 0.3 µm is obtained. Some preliminary tests showed evolution of the CHF values with the number of boiling crises (dry-outs) undergone. For a few dry-outs, the CHF values are very variable, and not always monotonous. The phenomena stabilizes for about 20 to 30 dry-outs. A comparable ageing process was mentioned by (Spencer, 2016) who observed that at least 20 hours of intense nucleate boiling on the surface were necessary to reach an almost stable value of the heat flux. A comparable trend was observed by (Mei et al., 2018) who noticed an increase of the CHF with the time of operation or the number of runs. This was attributed to corrosion and it is a different increase factor if the material is copper or steel. As the objective of the present work is to evaluate the influence of tilting angle and ball diameter on the CHF value, a stable reference was needed, and the surface was "aged" by submitting the heated plate to several boiling crises until stabilization was achieved. This reference state then enables the comparison of the different conditions tested (ball diameters, tilting angle). But it must be pointed out that this reference surface condition is not the "mirror polished" condition often met in literature. In order to avoid non-relevant comparisons, the influence of the different parameters of interest is then expressed through CHF ratios (with respect to the "reference" surface condition). The reference condition is an aged surface, at 90° tilting angle (vertical surface) and for a bed made of 4 mm balls.
Prior to any test, the water contained in the outer tank is electrically heated until isothermal conditions are reached in the ball bed and in the test section structures. Water is maintained at saturation temperature for at least 30 minutes to remove all dissolved gases. In order to avoid heat sinks, the heated plate and potentially the steam generator are simultaneously heated up to saturation temperature. The heated plate power is then maintained constant for at least 20 or 30 minutes to ensure steady state initial conditions to the forthcoming power ramp. The heating power is linearly increased up to the conditions of boiling crisis. The power increase is slow enough (0.09 W/s) to ensure quasi-static conditions. The CHF is considered as achieved when the heat flux decreases and the surface temperature strongly increases whereas the power keeps rising.

5. RESULTS

5.1. Test section effect and heated plate effect

Two identical heated cylinders are used to perform the tests in the "VP" section (without steam generator) and the "SG" section (with steam generator). In the same conditions (i.e. without steam production) and for a given heated cylinder, different CHF values are obtained in the two sections and thus cannot be inter-compared. An explanation to this test section effect may be the slightly different geometry of the bed in the two sections which is the same in width and thickness but not in height (see Fig. 6). This difference can create different convection loops in the test sections and affect CHF values. Considering the internal dimensions of these sections' ball bed, their cross section is 17280 mm^2.

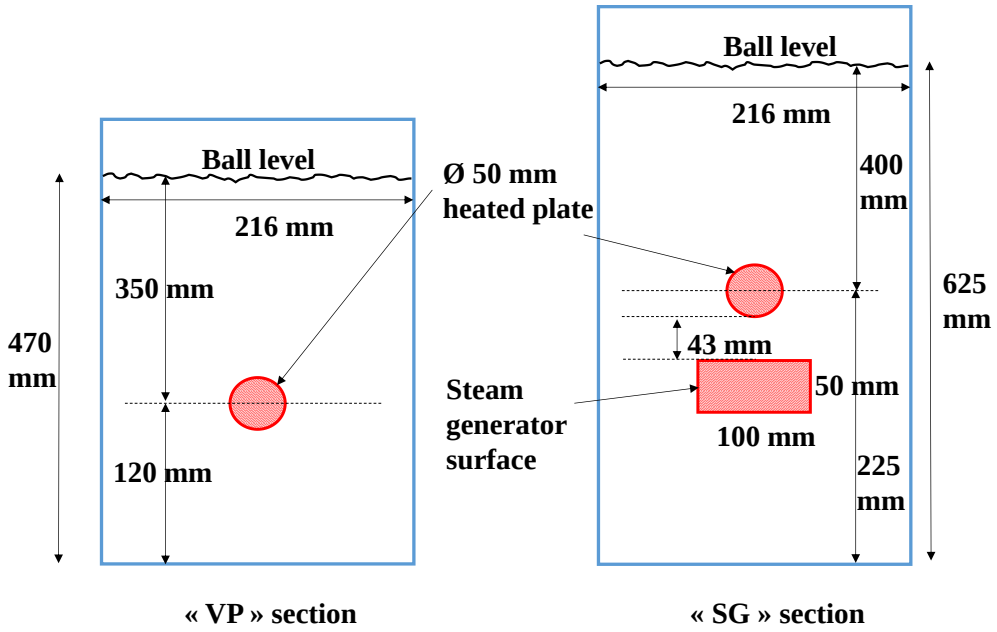

Figure 6. Internal Dimensions of the Ball Bed of VP Test Section (Left) and SG Test Section (Right).

Moreover, a heating cylinder effect has been evidenced. In a given test section, the CHF values are different depending on the cylinder used. For example, in "VP" test section, for 4 mm diameter balls and the heated plate positioned vertically, heated plate P10 gives a CHF about 250 kW/m^2 whereas heated plate P11 gives 210 kW/m^2.
As the two samples come from a single copper rod and have been controlled as geometrically identical, with exactly the same instrumentation, no explanation was found for such difference.
So in order to supply reliable results, the CHFs values are provided as effect ratios for a given test section and for a given heating cylinder.

5.2. Spreading of the Results

In spite of the surface aging process performed prior to the tests, some dispersion of the results was sometimes observed. When it was so large that it prevented consistent measures, the ball bed was vibrated[1] and the variability was reduced. Despite these precautions, some spreading may persist. Reasons for such spreading have not been clearly identified but may be in relation with global and local fluid conditions in the section. At the scale of the entire section, global convection loops may vary due to hydraulic instabilities. Close to the heated plate, local variations in the positions of each ball may be induced by liquid water or steam/bubbles convection movements, especially for small balls, and modify the ball-to-ball or ball-to-wall contact and the local fluid path. The local arrangement of balls may also be modified in experimental process, for example if the ball bed is re-filled. The presence of a greater void against the surface would lead to a higher local CHF. And for large tilting angle, the balls may locally lose contact with the heated plate and also result in a higher CHF. Most of these reasons being uncontrollable, a certain amount of dispersion is unavoidable and is counterbalanced by the numerous tests performed in each configuration of ball size, tilting angle and vapor rate.

[1] When the bed is vibrated, the bed porosity falls from about 0.36 to about 0.33. These values were mesured on a dedicated test section.

5.3. Results

The results are shown :
- on Fig. 7, for the CHF values obtained for **4 mm balls** in section "VP" (left) for tilting angle impact and in section "SG" (right) for tilting angle and steam flowrate impact, with heated plates P11 and P10 respectively.
- on Fig. 8, for the CHF values obtained for **2 mm balls** in section "VP" (left) for tilting angle impact and in section "SG" (right) for tilting angle and steam flowrate impact, with heated plate P11.

On all these figures, the x-axis title "heated plate dry-out number" indicates the number of the successive dry-outs undergone by the considered heated plate.
These figures show the effect of tilting angle and steam flowrate.

An additional series of tests were conducted to study the effect of liquid flowrate, in combination with tilting angle and steam flowrate. The related figures are shown in the dedicated paragraph.

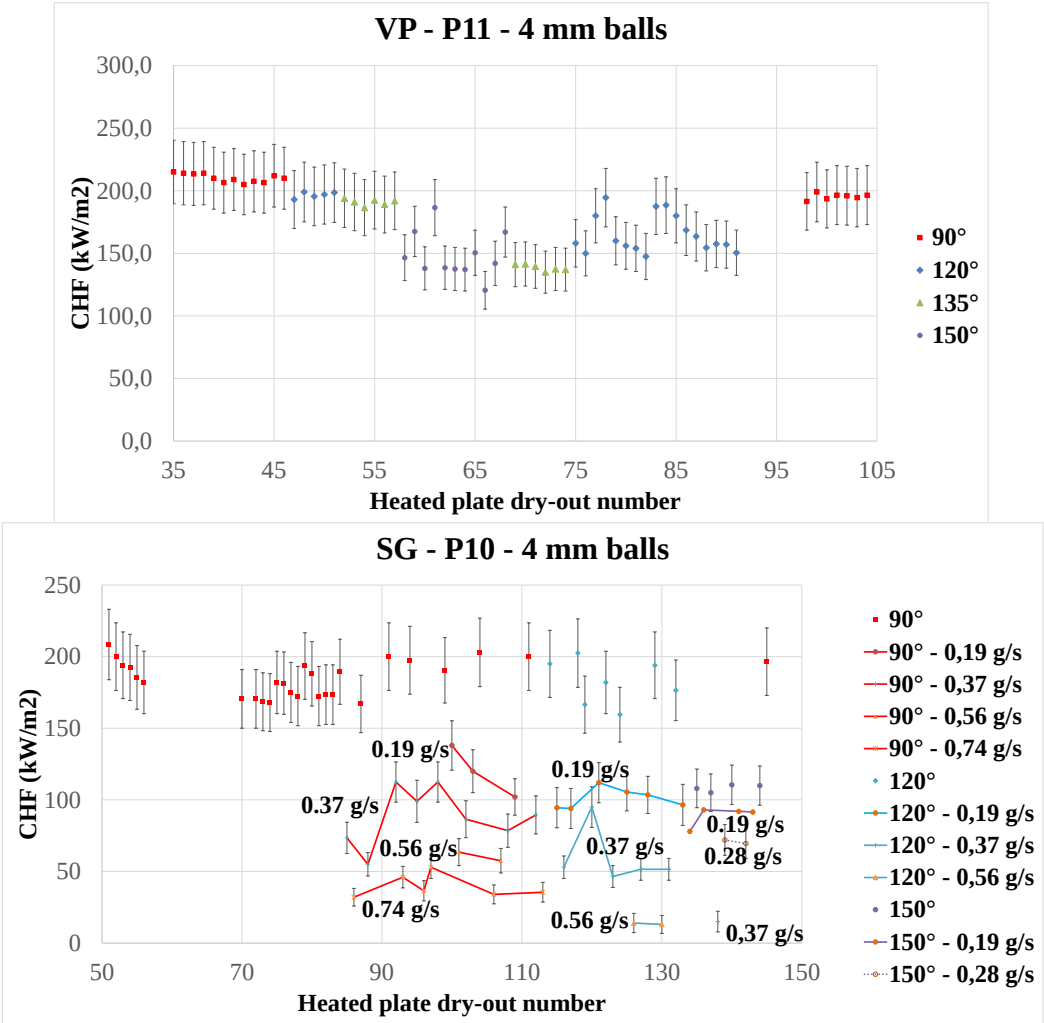

Figure 7. CHF Values Obtained with 4 mm Diameter Balls in Section "VP" with heated plate P11 (Above) and in Section "SG" with heated plate P10 (Below).

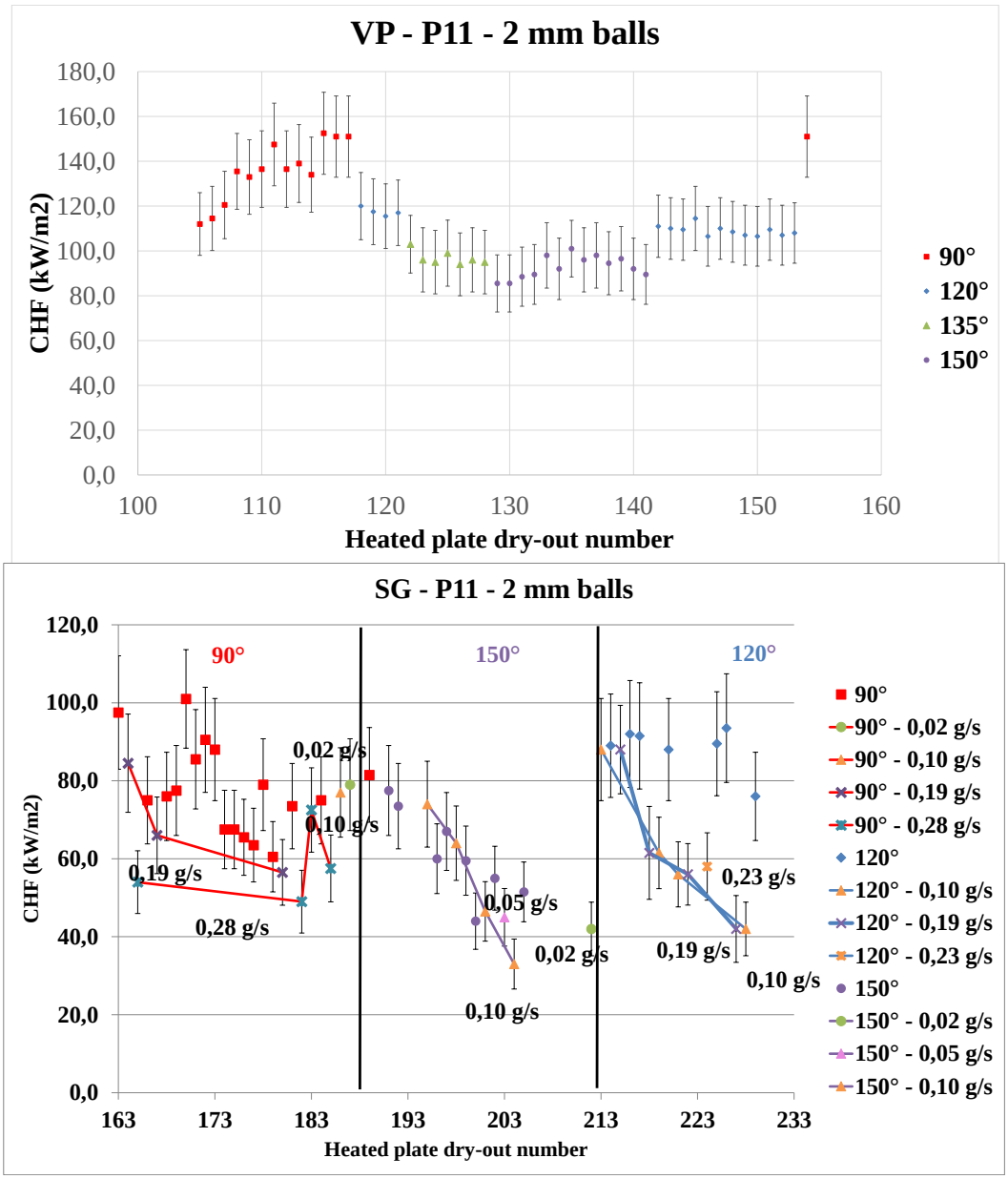

Figure 8. CHF Values Obtained with 2 mm Diameter Balls in Section "VP" with heated plate P11 (Above) and in Section "SG" with heated plate P11 (Below).

5.4 Tilting Angle Impact

It appears from Fig.7 and 8 that the impact of tilting angle is moderate. For 4 mm diameter balls, the tilting angle is a bit more influential for 150°. In section "VP", a strong dispersion is observed for 150° CHFs which might be explained by a slight local loss of contact of the balls on the surface, due to the large tilting angle.

For each tilting angle, the CHF values have been averaged and Fig. 9 shows the CHF decrease ratio with tilting angle (considering 90° as the reference angle):

$$Tilting\ angle\ CHF\ ratio = \frac{CHF(\theta)}{CHF(90°)} \quad (3)$$

As a "section effect" has been evidenced (see paragraph 5.1), the CHFs obtained in the two test sections are shown independently. Fig. 9 gathers 2 mm and 4 mm diameter balls results.
From the results shown in Fig. 9, it is not possible to derive an accurate correlation. Therefore we will simply consider that the CHF value decreases with $\sin\theta$ because $(\rho_l - \rho_s)g\sin\theta$ is the driving force acting on the steam phase to remove it from the heated surface. But Fig. 9 also shows that it does not tend towards zero for a downwards facing heated plate. It goes down to a minimum value which seems to be of the order of half of the reference value (for a given diameter).

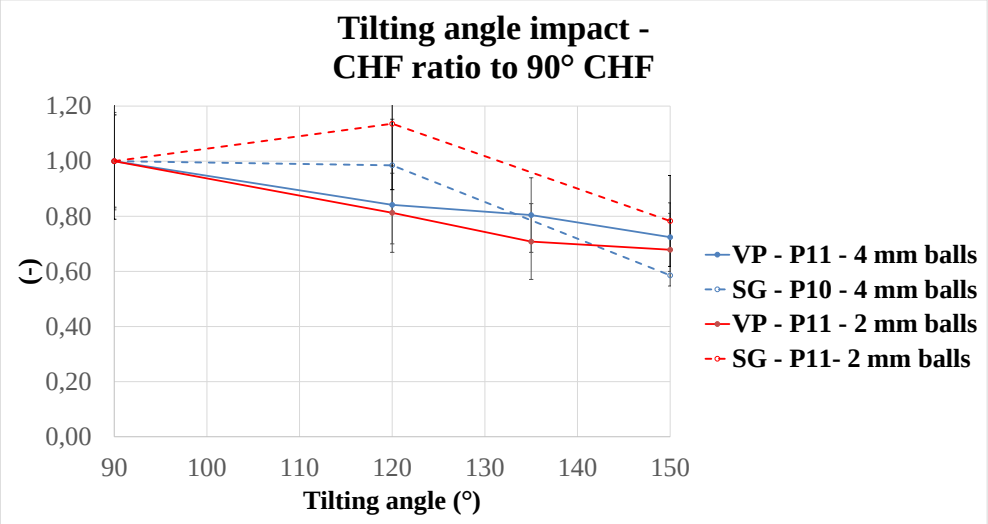

Figure 9. Tilting Angle Impact – CHF Ratio to 90° CHF for a Given Ball Diameter.

5.5 Steam Flowrate Impact

Unlike the tilting angle, the steam flowrate is highly influential and CHFs quasi equal to zero may be reached (see Fig. 7 and 8). For example, a flowrate of 0.74 g/s (corresponding to a SG power of 2000 W) in a 4 mm diameter ball bed leads to a CHF divided by four for a vertical surface.
For 2 mm diameter balls, the influence of the steam flowrate is much less visible, in particular for a tilting angle of 150° where the effect of steam flowrate seems hidden by the spreading of results. An explanation may be the small size of the balls for which capillary effects would not be negligible any more. The small cavities formed between the balls and close to the surface may retain the liquid and prevent steam circulating as it does for larger ball diameters.
For each experimental steam flowrate, the CHF values have been averaged and Fig. 10 shows the CHF decrease ratio with flowrate considering zero as the reference flowrate:

$$Steam\ flowrate\ CHF\ ratio = \frac{CHF(Q_{Steam})}{CHF(Q_{Steam}=0)} \quad (4)$$

One curve is derived for each ball diameter and each tilting angle.
It is interesting to compare these results with the ones obtained in (Spencer, 2016). In his experiments, a heat flux is applied over a height of 600mm, which results in a monotonous increase of the steam flow rate with the elevation. When the applied heat flux is uniform, it may be assumed that the steam mass

flow rate increases linearly with elevation. In that case, (Spencer, 2016)proposes a correlation where the CHF value decreases linearly with elevation,

$$CHF(Q_{Steam}) = CHF(Q_{Steam} = 0) - Kz \quad (5)$$

So, from Spencer results, we can conclude that the CHF value decreases with steam mass flow rate as $(1 - Q_{Steam})^a$ where a is an exponent which seems to be of the order 0.5 but there is a large uncertainty in Spencer's correlation because of an uncertainty on the exact location of dry-out. In our results, as illustrated in Fig. 10, the dependency seems to be more linear. This means that the exponent is closer to 1, or even a bit larger for the 4 mm balls. For the 2 mm balls, a correlation seems more difficult to derive but an approximation with a linear decrease seems reasonable. It is reminded that the results for a tilting angle of 150° cannot be considered as reliable as the others.

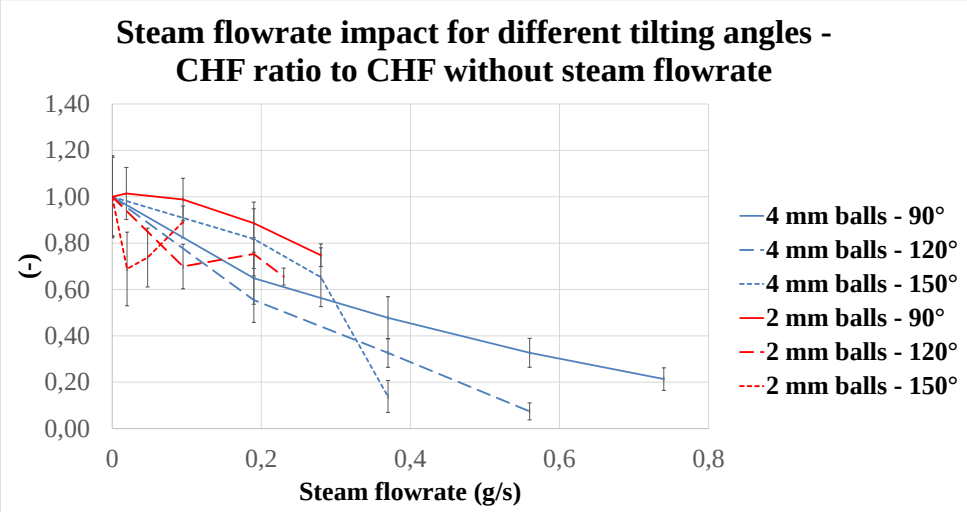

Figure 10. Steam Flowrate Impact for Different Tilting Angles - CHF Ratio to CHF without Steam Flowrate for a Given Ball Diameter.

5.6 Liquid Flowrate Impact

The liquid flowrate impact has been studied afterwards with an additional series of tests. These tests have been conducted in SG test section with heated plate P11, for the two ball diameters, for different tilting angles, with or without steam flowrate. As explained in the introduction, no published data were found for a comparable configuration of a heated plate in contact with a porous bed of balls, where the CHF was measured, as a function of inlet liquid flow rate. From a theoretical point of view, the works of (Wang & Beckermann, 1993a, 1993b) where they show that the non-dimensional CHF varies as the square root of the Peclet number where both non-dimensional numbers use the capillary diffusion coefficient. The CHF is shown to vary as :$CHF \propto Pe^{\frac{1}{2}} \propto j_l^{\frac{1}{2}}$ (7)

It is interesting to mention some works performed with bottom facing plates and an imposed water flowrate, but without the presence of balls. (Trojer et al., 2018) find a correlation where the CHF depends on $j_l^{\frac{1}{3}}$ and another correction term which is also a function of j_l. Another group performed experiments

(Kam et al., 2018) and developed a model (Yoon et al., 2019) where they found that the CHF depends on $j_l^{\frac{1}{3}}$, exactly as in (Trojer et al., 2018).
The results of the present experiment are shown on figure 11 for 4 mm balls and on figure 12 for 2 mm balls. One figure is given for each tilting angle. On all these figures, the x-axis is the liquid flowrate and the y-axis shows the ratio of CHF to the CHF value without liquid or steam flowrate. The steam flowrate is a parameter. Its values were chosen to reach the maximum possible one without SG dry-out, therefore they are different for 2 mm and 4 mm balls, and for a 150° tilting angle. For each case (ball diameter, tilting angle, liquid and steam flowrates), at least two tests were performed and each point represents the average.

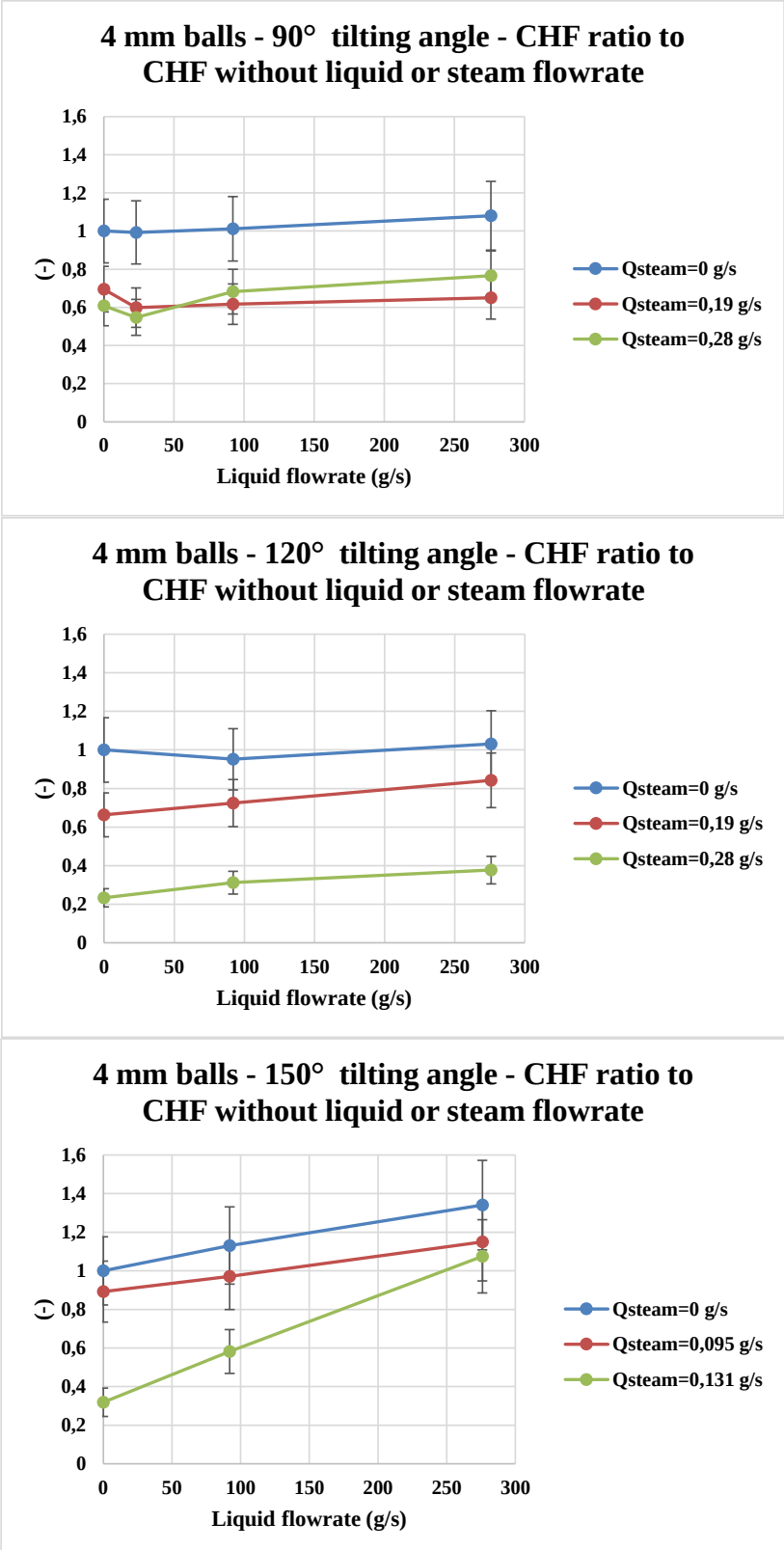

Figure 11. Liquid Flowrate Impact for Different Tilting Angles for 4 mm balls - CHF Ratio to CHF without Liquid or Steam Flowrate.

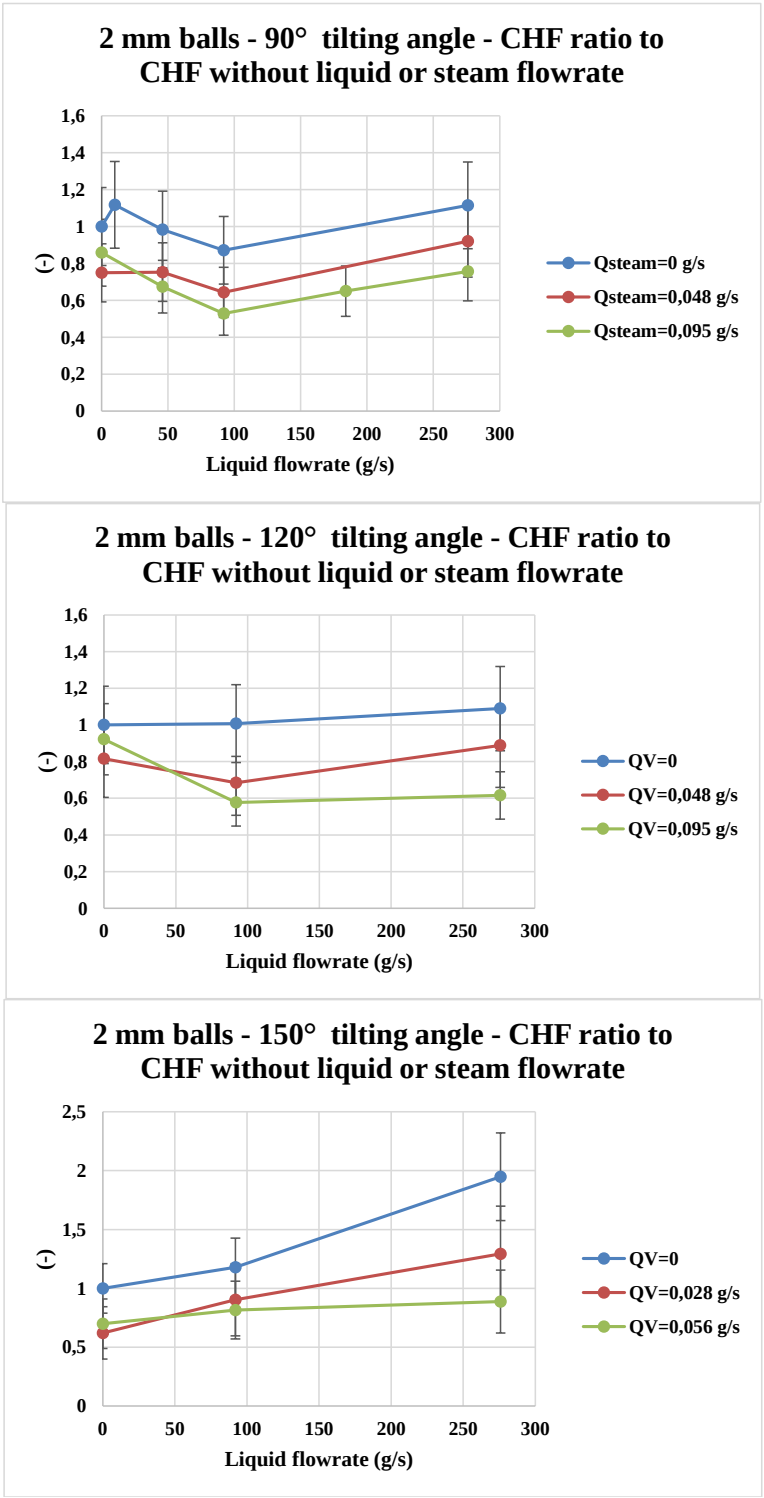

Figure 12. Liquid Flowrate Impact for Different Tilting Angles for 2 mm balls - CHF Ratio to CHF without Liquid or Steam Flowrate.

It appears from Fig. 11 and 12 that the increase of liquid flowrate slightly increases the CHF value in most cases. This effect seems to be more pronounced for a tilting angle of 150° (near horizontal), for the

highest tested steam flowrate for 4 mm balls and for no steam flowrate for 2 mm balls. Obviously, the dependency is not as $j_l^{\frac{1}{3}}$, as found for situation without balls. It looks more linear in most cases but there are not many points to really catch a possibly slightly non linear trend.
We can also point out that in some cases, the CHF may not be monotonously increasing with the liquid flowrate, which is rather unexpected. It may first show a decrease whose extend seems more marked with non-zero steam flowrate for small balls and near-vertical angles. This phenomenon was first observed and more thoroughly investigated with the 2 mm ball tests at 90° for which more liquid flowrates values were tested. As a minimum CHF ratio was observed for a liquid flowrate of 92 g/s, this value was kept for the rest of the tests to perform.

These two remarks suggest cross-effects between the surface inclination, the steam flowrate, the liquid flowrate and the ball diameter, probably linked with the geometry of the facility and with the capillary effects preventing the steam to escape (see discussion below). In particular, producing steam near the wall, just upstream of the heated surface where CHF is measured, probably leads to a non-homogeneous distribution of steam at the level of the heated plate. Therefore, it is difficult to estimate how water and steam can really get mixed before reaching the heated plate. For this reason, it seems too difficult to draw a correlation for the results where the steam flowrate is non-zero. In case of zero steam flowrate, the results differ, depending on the diameter of the balls:

- for the 4mm balls, the impact of the liquid flowrate seems negligible, except for the 150° inclination where it is increasing.
- for the 2mm balls, the impact of the liquid flowrate is non monotonous for the 90° inclination, negligible for the 120° inclination and strongly increasing (linearly) for the 150° inclination.

This shows that the liquid flowrate increases the mobility of the gas bubbles, especially when the gravity effect is small (near horizontal plate). However, the unexpected behavior observed for the vertical inclination and 2mm balls indicates a non linear behavior of the two-phase pressure gradient. Such non-monotonic behavior was already observed by (Tutu et al., 1984) and (Chikhi et al., 2016) who identified a decrease in the pressure drop for moderate void fraction. This indicates that a complex model with interfacial drag terms is necessary to explain the observed trend and that it is not possible to draw a simple correlation.

5.7 Ball Diameter Impact

For the tests performed in the same section with the same heated plate – that is to say in section “VP” with heated plate P11 – it has been possible to compare the results obtained with 2 mm diameter balls and 4 mm diameter balls. As the tilting angle was also investigated in this test section, it wass possible to draw the ratio CHF (2 mm) / CHF (4 mm) as a function of the tilting angle (see Fig. 11). For a vertical surface (tilting angle of 90°), the ratio is about 0.65 and seems rather constant with the tilting angle up to 150°.

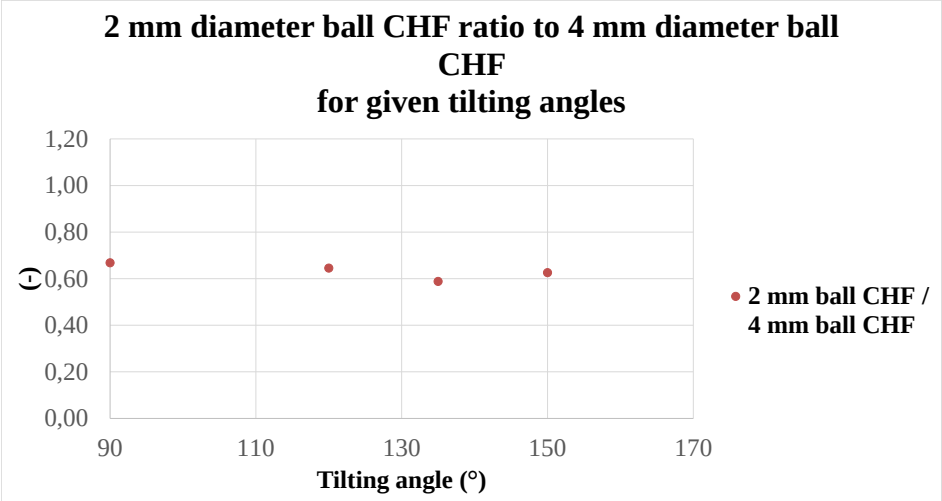

Figure 11. 2 mm diameter ball CHF ratio to 4 mm diameter ball CHF for given tilting angles (test section VP, heated plate P11).

This experimental ratio is close to a square root ball diameter ratio ($\sqrt{2}/\sqrt{4}\approx 0.71$).
This is consistent with one of the works of (Wang & Beckermann, 1993a, 1993b)where they show that the non-dimensional CHF varies as the square root of the Peclet number where both non-dimensional numbers use the capillary diffusion coefficient:

$$D_c = \frac{\varepsilon . K^{1/2} \sigma}{\nu_l} \tag{6}$$

Where K is the permeability which is proportional to d^2, d being the ball diameter.

In their model, the final expression gives:

$$CHF \propto K^{1/4} \propto d^{1/2} \tag{7}$$

The results obtained in our study seem to be more consistent with (Tung & Dhir, 1990)model for the CHF which is based on a flooding criterion where the square root of the ball diameter appears explicitely. However, the geometrical configuration is quite different (a sphere instead of a vertical plate) and it is difficult to assume that a similar counter-current flow limitation can be assumed.
Looking at the results from (Spencer, 2016), it appears that the CHF for a heated vertical wall and ball diameter of 11 mm is approximately 600 kW/m2: this means that the CHF value grows approximately linearly with the diameter, compared to the results obtained in our study for 4 mm balls. The reason for such change of behavior with diameter is probably the reduction of capillary effects with increasing pore size. In the recent study of (Spencer, 2022), a dependency with $d^{3/2}$is observed, for larger ball diameters. This indicates that there are probably several flow regimes according to the ball diameter, each regime leading to a different dependence with d.

6. DISCUSSION AND DERIVATION OF A CORRELATION FOR STEAM FLOWRATE EFFECT

From the analysis of our data and the comparison with previous data, we can conclude that there is a change of behavior in the nucleate boiling regime between 2 mm balls and 4 mm balls. Indeed, there are probably more capillary effects for smaller balls, as the Bond number decreases. As a reminder:

$$Bo = \frac{(\rho_l - \rho_s) g d^2}{\sigma} \quad (8)$$

For water and 4 mm balls, Bo ~1,5, and for water and 2 mm balls, Bo~0,38. For Bond numbers smaller than 1, capillarity effects are not negligible, which explains that the behaviors observed for 2 mm and for 4 mm balls differ.

The process of dry-out depends on the ability of steam to escape the heated surface and the ability of water to reach the surface. In the configuration that we studied, steam escape is driven by gravity and water flow to the wall is driven either by capillarity or by convection (Darcy regime). In the first case (water flow towards the wall driven by capillarity), dry-out is mostly dependent on the Bond number as in (Fukusako et al., 1986) and in (Wang & Beckermann, 1993a, 1993b), and in the second case (water flow towards the wall driven by convection) it is dependent on a modified Grashof number, as expressed in (Tung & Dhir, 1990). For 4 mm particles, with Bo close to 1, it is likely that both effects play a role and it is more difficult to model the process and find a suitable correlation.

As a result, we propose to derive a simple correlation for steam flowrate effect and inclination angle that agrees approximately with the data shown in this paper for the 4mm balls:

$$CHF = CHF_{ref} . \max[0; (1 - Q_{Steam})] . \max [0.5; \sin \theta] \quad (9)$$

The reference value is approximately $CHF_{ref} \sim 200 kW/m^2$ for a tilting angle of 90° (vertical heating plate) and for our "aged" heating plate surface.

7. CONCLUSION

The experimental apparatus presented in this paper allows to evaluate CHF for a copper surface in contact with a bed made of balls and de-ionized water. Different ball diameters, surface tilting angles, liquid and steam flowrates have been tested. Once the tested surface has been aged, the results remain relatively scattered. Several explanations are suggested for this phenomenon. Most of them are related to global or local convection loops and capillary effects. The present work shows that the influence of the surface tilting angle is relatively low whereas the influence of the steam flowrate is large. The impact of liquid flowrate is generally low except for the near horizontal inclination where the liquid flow can significantly contribute to increase the CHF. The ball diameter impact is the same irrespective of the tilting angle in the studied range and seems to vary with the square root of the ball diameter.

Correlations have been derived for tilting angle impact and steam flowrate impact. These correlations are now ready to evaluate the maximum size of a stabilized corium pool in a debris bed. For the liquid flowrate, no obvious and simple correlation could be found and it was not in agreement with existing models.

ACKNOWLEDGMENTS

The authors acknowledge Electricité De France (EDF) for their financial support.

REFERENCES

Broughton, J. M., Pui, K., Petti, D. A., & Tolman, E. L. (1989). Scenario of the Three Mile Island Unit 2 accident. *Nuclear Technology*, *87*(1), 34–53. https://doi.org/10.13182/NT89-A27637

Chikhi, N., Clavier, R., Laurent, J. P., Fichot, F., & Quintard, M. (2016). Pressure drop and average void fraction measurements for two-phase flow through highly permeable porous media. *Annals of*

Nuclear Energy, *94*, 422–432. https://doi.org/10.1016/j.anucene.2016.04.007
Coindreau, O., Fichot, F., & Fleurot, J. (2013). Nuclear fuel rod fragmentation under accidental conditions. *Nuclear Engineering and Design*, *255*, 68–76. https://doi.org/10.1016/j.nucengdes.2012.09.021
Fukusako, S., Komoriya, T., & Seki, N. (1986). An experimental study of transition and film boiling heat transfer in liquid-saturated porous bed. *Journal of Heat Transfer*, *108*(1), 117–124. https://doi.org/10.1115/1.3246875
Kam, D. H., Choi, Y. J., & Jeong, Y. H. (2018). CHF experiment with downward-facing carbon and stainless steel plates under pressurized conditions. *International Journal of Heat and Mass Transfer*, *125*, 670–680. https://doi.org/10.1016/j.ijheatmasstransfer.2018.04.026
Mei, Y., Shao, Y., Gong, S., Zhu, Y., & Gu, H. (2018). Effects of surface orientation and heater material on heat transfer coefficient and critical heat flux of nucleate boiling. *International Journal of Heat and Mass Transfer*, *121*, 632–640. https://doi.org/10.1016/j.ijheatmasstransfer.2018.01.020
Park, H. M., Jeong, Y. H., & Carnevali, S. (2018). Critical heat flux model on a downward facing surface for application to the IVR conditions. *Nuclear Engineering and Design*, *330*(January), 317–324. https://doi.org/10.1016/j.nucengdes.2018.02.006
Rougé, S. (1997). SULTAN test facility for large-scale vessel coolability in natural convection at low pressure. *Nuclear Engineering and Design*, *169*(1–3), 185–195. https://doi.org/10.1016/s0029-5493(96)01277-0
Spencer, J. (2016). Measurement of Critical Heat Flux in a Candu End Shield Consisting of a Vertical Surface Abutting a Packed Bed of Steel Shielding Balls. *CNL Nuclear Review*, *6*, 1–12. https://doi.org/10.12943/cnr.2016.00002
Spencer, J. (2022). Critical heat flux in a CANDU end shield – Influence of shielding ball diameter. *Nuclear Engineering and Technology*, *54*(4), 1343–1354. https://doi.org/10.1016/j.net.2021.10.008
Sulatskii, A. A., Cherny, O. D., Efimov, V. K., & Granovsky, V. S. (1997). Boiling Crisis at the Outer Surface of VVER Vessel. *Proceedings of International Symposium on the Physics of Heat Transfer in Boiling and COndensation*.
Trojer, M., Azizian, R., Paras, J., McKrell, T., Atkhen, K., Bucci, M., & Buongiorno, J. (2018). A margin missed: The effect of surface oxidation on CHF enhancement in IVR accident scenarios. *Nuclear Engineering and Design*, *335*(May), 140–150. https://doi.org/10.1016/j.nucengdes.2018.05.011
Tung, V. X., & Dhir, V. K. (1990). Experimental Study of Boiling Heat Transfer From a Sphere Embedded in a Liquid-Saturated Porous Medium. *Journal of Heat Transfer*, *112*(3), 736. https://doi.org/10.1115/1.2910448
Tutu, N. K., Ginsberg, T., & Chen, J. C. (1984). Interfacial drag for two-phase flow through high permeability porous beds. *J. of Heat Transfer*, *106*, 865–870.
Wang, C.-Y., & Beckermann, C. (1993a). A two-phase mixture model of liquid-gas flow and heat transfer in capillary porous media-I. Formulation. *International Journal of Heat and Mass Transfer*, *36*(11), 2747–2758. https://doi.org/10.1016/0017-9310(93)90094-M
Wang, C.-Y., & Beckermann, C. (1993b). A two-phase mixture model of liquid-gas flow and heat transfer in capillary porous media-II. Application to pressure-driven boiling flow adjacent to a vertical heated plate. *International Journal of Heat and Mass Transfer*, *36*(11), 2759–2768. https://doi.org/10.1016/0017-9310(93)90095-N
Yoon, J., Kam, D. H., Park, H. M., & Jeong, Y. H. (2019). CHF correlation development under ERVC conditions by using the local liquid velocity from PIV measurements. *International Journal of Heat and Mass Transfer*, *128*, 171–184. https://doi.org/10.1016/j.ijheatmasstransfer.2018.08.127